Supporting Information for:

Characterization of Ultrafine Particulate Matter from Traditional and Improved Biomass Cookstoves

Brian Just[a,], Steven Rogak[a] and Milind Kandlikar[b,c]*

[a] Department of Mechanical Engineering, The University of British Columbia, 6250 Applied Science Lane, Vancouver, BC, V6T 1Z4

[b] Institute for Resources, Environment and Sustainability, The University of British Columbia, 2202 Main Mall, Vancouver, BC, V6T 1Z4

[c] Liu Institute for Global Issues, The University of British Columbia, 6476 NW Marine Dr, Vancouver, BC, V6T 1Z2

The Supporting Information contains 11 pages (including title page), 8 figures, and 3 tables.

*Corresponding author e-mail: bgjust13@gmail.com.

Method section

SI 1: Additional notes on stoves, fuel, and procedure

The three-stone baseline consisted of three bricks (57 mm x 92 mm x 194 mm) placed in symmetrical orientation with the cooking pot resting at an elevation of 92 mm.

All hemlock pieces were cut on the dame day and stored in identical manner and testing occurred over a minimal period of time. Moisture content was measured by drying fuel samples at 105ºC until mass no longer decreased. An elemental analysis was based on testing 5 mg of shavings from several sticks. For the pellets, carbon content was based on 5 mg of pulverized powder from a random sampling of pellets.

The exhaust system was constructed in an engine test cell at the Clean Energy Research Centre (CERC) at The University of British Columbia. A single-speed blower extracted exhaust at ~190 scfm; mixing baffles at the exhaust duct inlet ensured adequate mixing of combustion products with dilution (room) air. Natural dilution occurred as combustion products mixed with ambient air before entering the exhaust hood; a dilution ratio of 150:1 was estimated by comparing measured oxygen to the amount of oxygen required for stoichiometric combustion of measured CO_2 and CO. Prior to testing, a smoke tube was used to verify that exhaust flow rate and hood geometry, including vertical length and the size of the hood access opening, allowed for capture of all combustion products; hood height was adjusted so that plume velocity at the average stove height was near the range recommended by Ballard-Tremeer and Jawurek ([1]).

Preliminary tests were conducted with each cookstove to learn about optimal ignition and fuel loading techniques. Early testing of the Chulika indicated an initial burn period characterized by high, unstable PM mass emissions; starting with fresh fuel it took about 20 minutes to reach a relatively stable condition in which the fire is maintained by a mix of charred and fresh fuel. Following the "warm-up" period, for the Chulika cookstove a continuous four-stick burn (as in Figure S1, reproduced here from Figure 1(b) in the main article) was tended for 60 minutes.

Figure S1. Chulika cookstove four-stick burn.

After each Chulika test, all char and unburnt fuel was transferred to a three-stone fire. This shortened the startup phase, after which the three-stone fire was tended in similar manner for 60 minutes. Oorja performance was notably influenced by the starting temperature of its insulated combustion chamber (see also SI 8). For this reason, tests for both improved stoves occurred after a sufficient cool-down period (3-4 hours minimum).

PTFE filter samples were stored for a minimum of 24 hours in a climate-controlled room (at 21 ± 2°C and 40 ± 5% RH). Filters and a set of controls were charge-neutralized using a Po-210 source and weighed three times before and after aerosol collection. Filter masses were combined with collection time and known rate of flow (via calibrated critical orifice) to determine mass of PM per volume of exhaust air. A dynamic blank was collected and measured with the same protocol and was subtracted from the results with an adjustment for its collection time. DustTrak-predicted filter loading was calculated by combining an integration of its 1 Hz readings during the period of filter collection (or using its average value) with flow rate through the filter.

Quartz filters were pre-baked at 700°C for one hour in order to remove carbon contamination. Before and after tests, filters were stored in 47mm diameter plastic containers and wrapped in foil; they were frozen prior to shipment for analysis. 1.50 cm x 1.00 cm sections of filters were analyzed. All were corrected for positive OC artifact by subtracting OC content of a quartz filter behind a PTFE filter taken in parallel at the same time that aerosol was collected on the primary quartz filter.

Procedure PTFE and quartz filter blanks were collected, with (small) adjustments to reported results.

The AVL CEB II Emissions Bench was calibrated each day of testing; residence time in the line was approximately 15 seconds. The line was heated to prevent condensation. A second CO_2 line from a location outside of and adjacent to the exhaust hood was routed to a second CO_2 sensor for a continuous background CO_2 measurement. Net CO_2 from combustion also included a correction based on the (small) difference in readings between the two CO_2 sensors during background testing.

The TSI DustTrak DRX Aerosol Monitor 8533 was calibrated with Arizona Road Dust and assumed a constant refractive index, so errors were present when composition and size varied from the calibration material. Since relative humidity (RH) may affect scattering signal, water was changed once per test to prevent boiling.

Scan time for the SMPS and APS was set to 135 seconds and the Magee Scientific Aethalometer Model AE 21 was set to a 60-second sampling period.

Exhaust temperature and relative humidity were measured before and after each testing period by a LabJack EI-1034 digital capacitive sensor. Exhaust flow rate was monitored continuously by a Nailor Ampliflow 36FMS-06 airflow sensor connected to a Dwyer MS-121-LCD differential pressure sensor; this was calibrated using a tracer gas prior to testing. An auxiliary silicon temperature sensor (LabJack EI-1050) measured water temperature in the cooking vessel in case of future interest. Video of stove flames was captured for later synchronization with data if needed. Clocks for all instruments and data logging PCs were synchronized before each day of testing. During tests, the emissions bench, DustTrak, aethalometer, and auxiliary instruments recorded continuously.

SI 2: TPS schematic
The thermophoretic particle sampler (TPS) used thermophoresis to deposit particulate matter onto a 3.05mm diameter transmission electron microscopy (TEM) grid. The aerosol stream was heated via power applied to a 32 gauge Nichrome wire wrapped around a ceramic-coated

hypodermic needle. Sensitive and heated parts are contained within a robust, insulating Delrin body; see Figure S2.
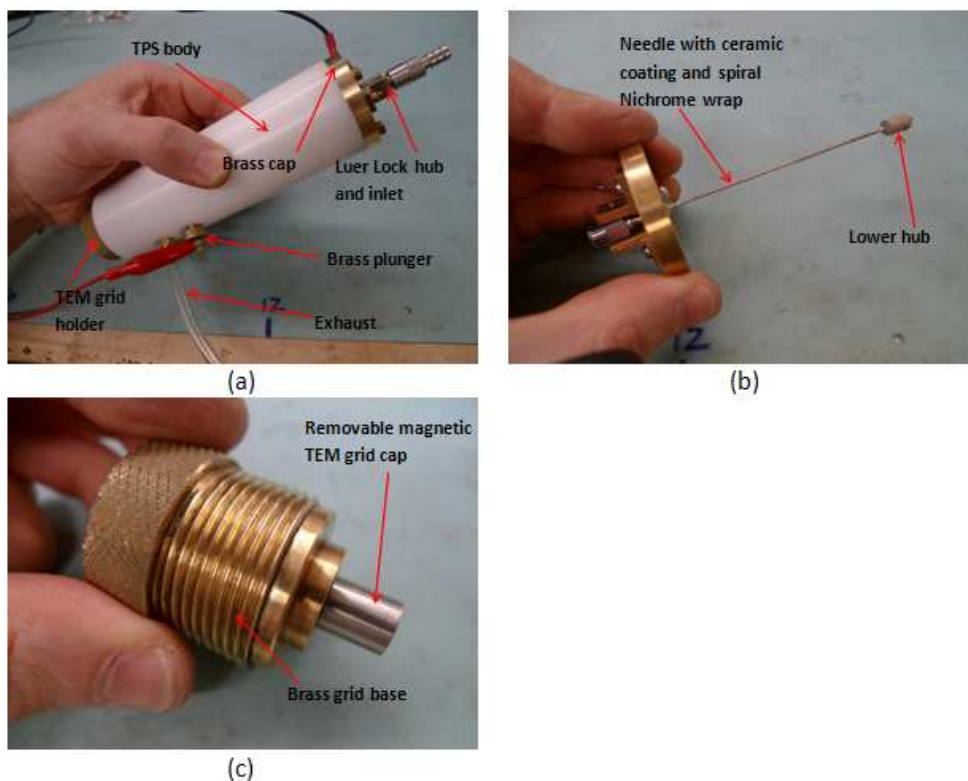

Figure S2. TPS overview: (a) TPS body with electrical connections, (b) internal needle assembly, (c) TEM grid holder

Results section

SI 3: Determination of "steady" burn period
The rate of CO_2 emissions was not an effective measure of steadiness since it is a measure of carbon combustion rate and not "maturity" of the fire and real-time PM is largely dependent on fueling and fuel tending. Rather, the steady burn period was defined by noting SMPS size distributions. For a given stove / test, PM mode size displayed time dependence. After the initial combustion period, size distribution stabilized and further scans yielded similar results despite irregularities associated with fueling. This "stabilization" is best indicated by an example. In Figure S3, dark dashed lines indicate the first five SMPS scans (after cookstove ignition) for one Chulika cookstove test; unbroken lines show all subsequent scans, which are scattered randomly with no clear time-based trend. In this example, we defined the steady data period to begin with the sixth SMPS scan. The term "steady" is used here, but this implies only that the time dependent variation is minimized. Considerable variations in emissions still occur, but by averaging a number of scans over a range of tests, repeatable results can be reported (see also SI 5).
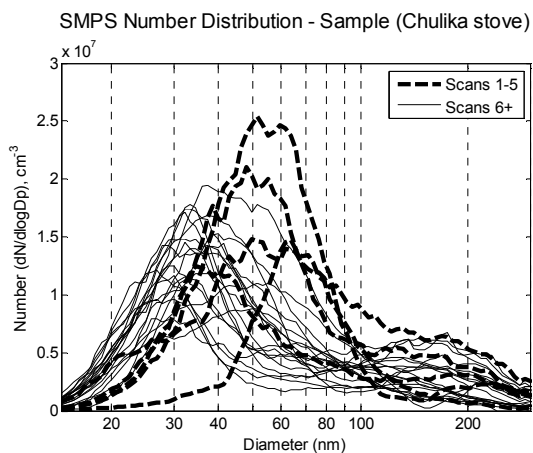
Figure S3. Example SMPS scan summary

SI 4: Sample of real-time representative results

Figure S4 displays PM, CO_2 and CO levels from a 1500-second steady-burn period for each. CO_2 is shown as a comparative measure of rate of combustion and dilution and was not normalized in this figure. The fact that data spikes for the three-stone and Rocket correlated to fire tending (adding / moving fuel) helps explain why emissions for the (batch-loaded) Gasifier appear smoother.
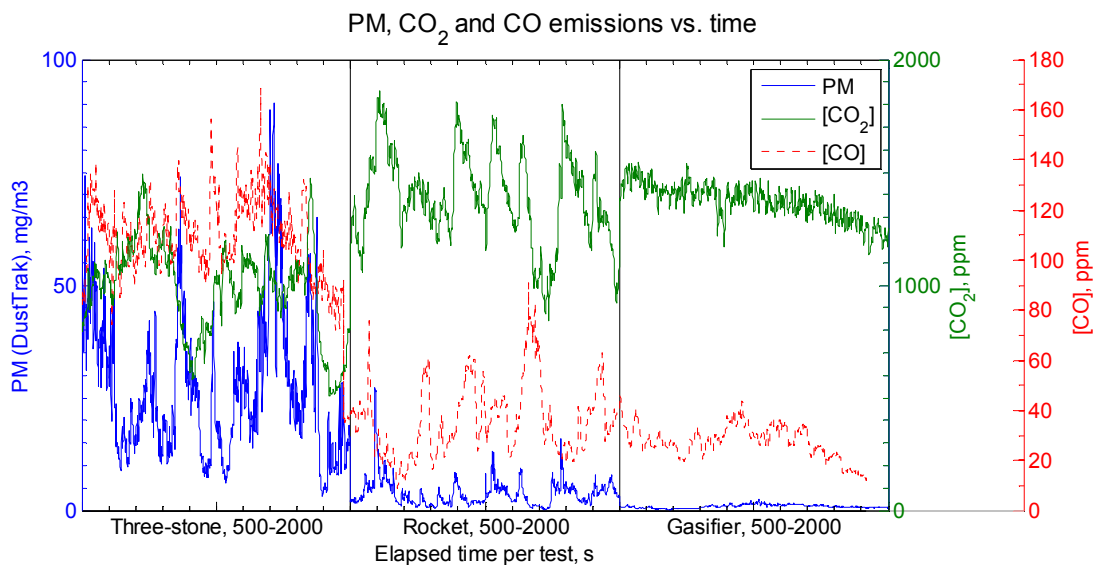

Figure S4. Sample of raw emissions data for a single test series

The ratio of CO_2 to CO can be used as a measure of combustion efficiency. As expected based on the time-series data in Figure S4, Figure S5 indicates increasing efficiency corresponding to the transition from three-stone to Rocket to Gasifier.
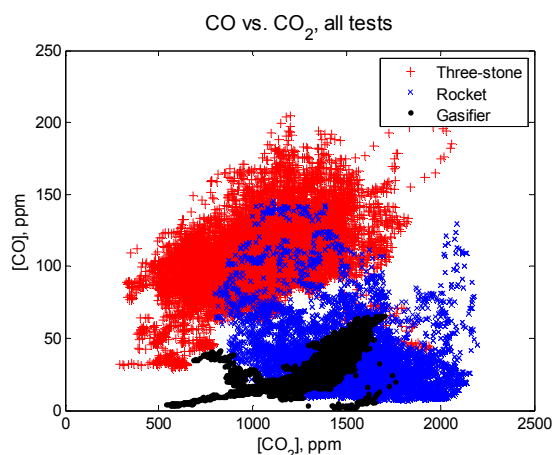
S5

Figure S5. CO vs. CO$_2$. One data point per second (12805 total) during all tests' "steady" period.

## SI 5: Notes on repeatability of SMPS scans

A breakdown of the tests that went into the creation of the SMPS number distribution summary (Figure 3 in the article text) gives an idea of the repeatability between tests on a given cookstove; see Figure S6. Individual lines represent the averages of all "good" scans for a test. Mode diameter is relatively consistent; the main difference between tests was amplitude (quantity of particles emitted).
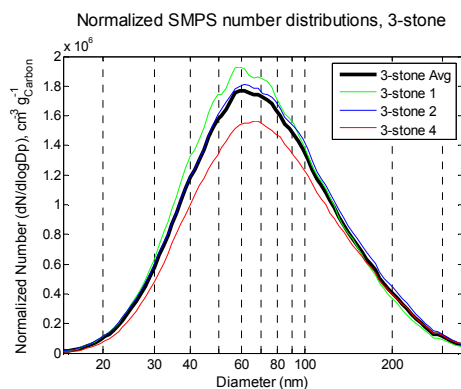
(a)
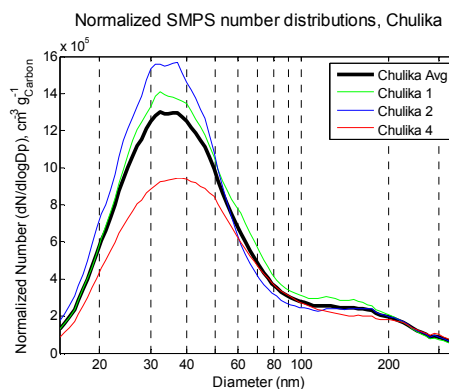
(b)
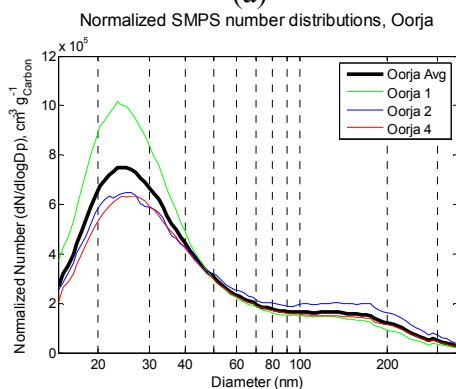
(c)

SI 6: Overview of combined SMPS/APS scans

The APS gives a single value for particle count in the ~0.35–0.52 um range and per bin values from 0.53-20 um. APS data is displayed alongside SMPS results in Figure S7.
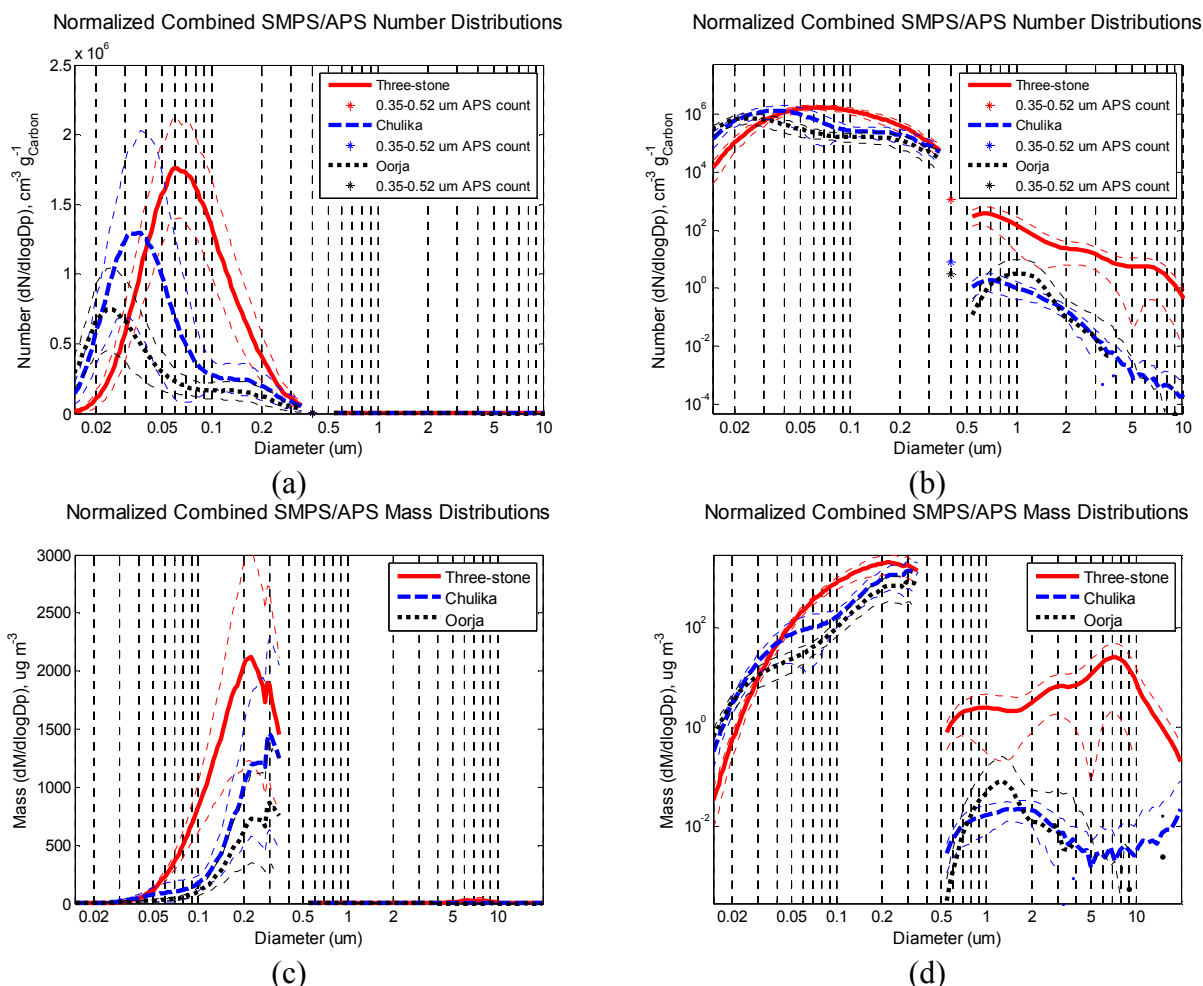

(a)

(b)

(c)

(d)

Figure S7. Normalized combined SMPS/APS distributions by number, (a) linear-log scale, (b) log-log scale, and mass (c) linear-log scale, (d) log-log scale.

SI 7: Additional notes on DustTrak "errors"

The DustTrak estimation "errors" indicated in the main article (172% overestimation for the three-stone fire, 21% overestimation for the Rocket, and 16% underestimation for the Gasifier) may be partially explained by the EC/OC results. Since the DustTrak estimates PM based on a light scattering, high OC (low EC) content may increase scattering relative to the calibration material (Arizona Road Dust) and result in overestimation; underestimation could accompany emissions of high proportions of (light absorbing) EC.

Given that scattering intensity is proportional to the sixth power of particle diameter, one may expect that emissions with larger particles (e.g., three-stone fire) would be over-predicted relative to cookstoves that produce smaller particles (e.g., the two improved stoves tested). Since the stove with the largest particles had the highest OC content (and vice versa), further tests would be required to determine the relative contributions of size and EC/OC content on scattering-based PM mass measurements.

## SI 8: Additional notes on Oorja operating modes

During June 2012 follow-up tests, the Low fan setting on the Oorja cookstove was used in accordance with the setting employed during the primary test series of March 2012. Likewise, an equivalent mass of pellets was used although they were from a different batch and neither carbon nor moisture content was tested. Environmental conditions in the (non-climate controlled) laboratory were also different (summer vs. winter).

During the first test, the flame was visibly lower than in previous tests; lower measured CO_2 emissions supported this observation. Interestingly, the SMPS traces Figure S8(a) were shifted right (larger number mode) compared to previous Oorja tests and PM mass emissions measured by the DustTrak were significantly higher than during the original (March 2012) tests. Partway through the next test (#2b, Figure S8(b)), the fan setting was switched from Low to High. In a third test (Figure S8(c)), the stove was started on High, switched to Low, and then turned back to High. From Figure S8(b,c), the correlation between particle size distribution and fan setting is very clear.

In initial preliminary tests with the Oorja cookstove, it was noticed that initial combustion chamber temperature significantly affected measured emissions; for this reason, tests were separated by breaks of several hours to allow complete cooling of the cookstove to laboratory ambient temperature.

Differing fuel, exhaust flow, and environmental conditions may account for the discrepancies between the March 2012 tests and the June 2012 follow-up tests.

Further study is warranted. Discrete operating conditions should be reproduced and emissions monitored in the same way as during the primary test series.
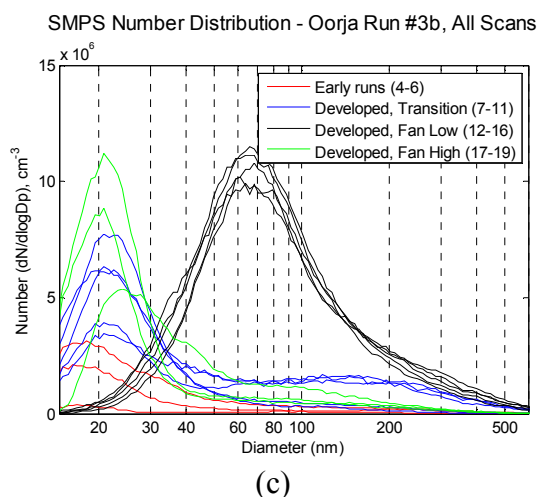

(a)

(b)

(c)
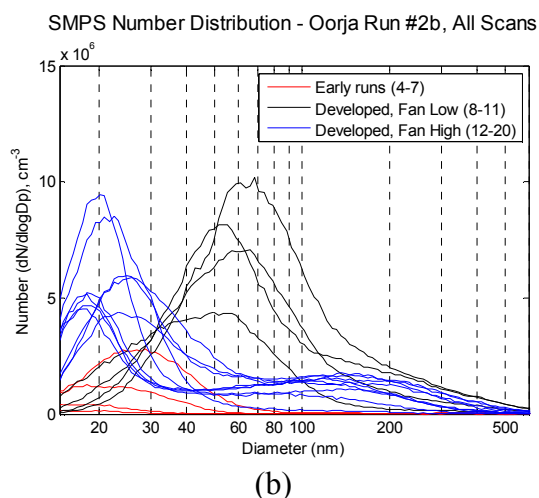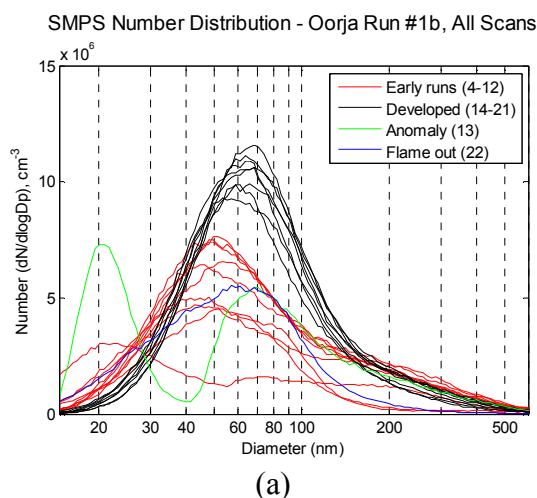
Figure S8. Oorja results from June 2012 follow-up tests

SI 9: TEM imaging protocol

TEM grids were collected for most test series; identification codes are indicated in Table S1. Collection time and averaged corrected DustTrak reading during collection time[1] are indicated in brackets and used for a comparative estimate of grid loading. Except where noted, pressure drop across the TPS was set to 1 psi corresponding to an estimated flow rate of 2.3 lpm. The number in bold is a "relative loading factor" normalized to the grid loading of Oorja Test 1 (D1) based on collection time, average corrected DustTrak reading, and TPS exhaust flow rate.

Table S1. TEM grid matrix

Stove	Test 1	Test 2	Test 4
Oorja	D1 [90s @ 2.01 mg/m^3] **1.00**	B9[a] [180s @ 0.49 mg/m^3] **0.48**	B6 [90s @ 2.12 mg/m^3] **1.05**
Chulika	D2 [45s @ 1.75 mg/m3] **0.44**	E1 [35s @ 7.29 mg/m3] **1.41**	B7 [60s @ 2.08 mg/m3] **0.69**
3-Stone	D4[b] 30s @ 11.73 mg/m3 **1.18**	E3[c] [10s @ 12.80 mg/m3] **0.43**	B8 [20s @ 9.57 mg/m3] **1.06**

[a] The grid taken during Oorja test #2 (D5) was lost. In lieu of the desire to study three grids per stove type, grid B9 from test series #5 was used for the Oorja.
[b] Second grid taken during this test because E1 (visually) appeared more heavily loaded than usual.
[c] TPS pressure drop is 0.5 psi, yielding an estimated 1.4 lpm.

---

[1] Based on overall average gravimetric correction, not from the specific test in question.

For each grid, five locations were chosen for magnification and imaging. The first step was to roughly center the grid in the microscope and record the coordinates; this location was Point #1. Not recorded are the stagnation / impact regions near the grid center[2]. Other points are located relative to Point #1 as indicated in Table S2. If the carbon film is damaged in the region of interest, the nearest (intact) adjacent grid location was used.

Table S2. TEM imaging coordinates (in um)

Point	Relative coordinates
1	(0, 0)
2	(+300, +300)
3	(-300, +300)
4	(-300, -300)
5	(+300, -300)

For each point, the nearest grid corner to the "right" (as viewed through the TEM camera, negative "x" in TEM coordinates) was located. The first image taken for each point (at lowest magnification, 15000x) shows a grid corner. Subsequent procedure is shown in Table S3.

Table S3. TEM imaging steps

Step	Magnification	Procedure
1	15000 x	Move to center, record reference coordinates, record image of nearest grid corner to "right".
2	50000 x	Zoom in further, keep centered.
3	150000 x	Focus on a region near the center that shows an agglomerate and adjacent smaller particles (if possible).
4	300000 x	Zoom in further, focusing on the region in Step 4.
5	500000 x	Zoom in further (optional, doesn't always provide useful information).

With only five imaging locations, counting was not done; rather, the goal was to look for trends and primary particle size between stove types.

SI 10: Additional notes on particles collected onto TEM grids
For all images it is possible that particles counted as components of agglomerates were actually independent particles that collided with an agglomerate on the TEM grid. Lower concentrations of spherical nanoparticles relative to the number of agglomerates were evident compared to that predicted by SMPS data (noting that the non-spherical nature of soot agglomerates means that

---

[2] The center of the stagnation region is an alternate way to "set" the zero reference for Point #1. However, on some grids it is not obvious to locate and it is frequently the site of broken carbon film.

aerodynamic diameter can be significantly smaller than mobility diameter, the basis of the SMPS measurement). This implies that many agglomerates may have deposited via impaction the (d_{50} cutoff diameter for impaction deposition in the TPS with the present operating conditions is ~300 nm based on based on aerodynamic diameter).

Cited literature for Supporting Information

(1)   Ballard-Tremeer, G.; Jawurek, H. H. The "hood method" of measuring emissions of rural cooking devices. *Biomass Bioenergy* **1999**, *16*.